

Silibinin Inhibits Tumor Growth through Downregulation of Extracellular Signal-Regulated Kinase and Akt *in Vitro* and *in Vivo* in Human Ovarian Cancer Cells

Hyun Jin Cho,^{†,‡} Dong Soo Suh,^{†,§} Soo Hyeon Moon,[§] Yong Jung Song,[§] Man Soo Yoon,[§] Do Yoon Park,^{||} Kyung Un Choi,^{||} Yong Keun Kim,[⊥] and Ki Hyung Kim^{*,§}

[‡]Department of Medicine, Graduate School of Medicine, Pusan National University, Busan 602-739, Korea

[§]Department of Obstetrics and Gynecology, Pusan National University School of Medicine, and Medical Research Institute and Pusan Cancer Center, Pusan National University Hospital, Busan 602-739, Korea

^{||}Department of Pathology, Pusan National University School of Medicine, and Medical Research Institute and Pusan Cancer Center, Pusan National University Hospital, Busan 602-739, Korea

[⊥]Department of Physiology, College of Medicine, Pusan National University, Busan 602-739, Korea

ABSTRACT: Anticancer activity of silibinin, a flavonoid, has been demonstrated in various cancer cell types. However, the underlying mechanisms were not elucidated in human ovarian cancer cells. The present study was undertaken to examine the effect of silibinin *in vitro* and *in vivo* on tumor growth in human ovarian cancer cells. Silibinin decreased cell viability in a dose- and time-dependent manner. Silibinin caused an increase in reactive oxygen species (ROS) generation, and the silibinin-induced cell death was prevented by the antioxidant *N*-acetylcysteine (NAC). Western blot analysis showed silibinin-induced downregulation of extracellular signal-regulated kinase (ERK) and Akt. Transfection of constitutively active forms of MEK and Akt prevented the silibinin-induced cell death. Oral administration of silibinin in animals with subcutaneous A2780 cells reduced tumor volume. Subsequent tumor tissue analysis showed that silibinin treatment induced a decrease in Ki-67-positive cells, an increase in transferase-mediated dUTP nick end labeling (TUNEL)-positive cells, activation of caspase-3, and inhibition of p-ERK and p-Akt. These results indicate that silibinin reduces tumor growth through inhibition of ERK and Akt in human ovarian cancer cells. These data suggest that silibinin may serve as a potential therapeutic agent for human ovarian cancers.

KEYWORDS: Ovarian cancer cells, silibinin, tumor growth, ERK, Akt

INTRODUCTION

Ovarian cancer is the most lethal of the gynecologic malignancies.¹ Because of a lack of effective biomarkers for screening, more than 70% of ovarian cancers are diagnosed at advanced stages and associated with high morbidity and mortality.² Although a moderate percentage of patients initially respond well to the first-line chemotherapy, recurrence is commonly observed. Recurrence is frequently accompanied by resistance to the platinum-based chemotherapy administered as first-line treatment.³ Therefore, novel anticancer agents, which operate via different mechanisms than that of platinum-based drugs, are required to improve outcomes for women with advanced ovarian cancer.

Flavonoids are common constituents of the human diet, present in fruits, vegetables, and medical herbs. Flavonoids can be divided into various classes according to their molecular structures; the main groups are flavanols, flavanones, flavonols, flavones, anthocyanins, and isoflavone.⁴ Recently, flavonoids have received much attention as potential chemopreventive and chemotherapeutic agents.^{5–7} Because currently available chemotherapeutic agents have serious side effects and drug resistance, their use is limited in cancer treatment. Flavonoids may be a very promising group of compounds exerting the chemopreventive and chemotherapeutic effects.

Silibinin, a flavonoid, is a major bioactive component present in silymarin isolated from the plant milk thistle (*Silybum*

marianum) and has been extensively used for its hepatoprotective effects in Europe and Asia. Recently, anticancer activities of silibinin have been demonstrated in various *in vitro* and *in vivo* cancer models.^{8–11} Silibinin has been reported to restore sensitivity to paclitaxel¹² and potentiate the activity of cisplatin¹³ in ovarian cancers. However, the anticancer efficacy of silibinin alone in both *in vitro* and *in vivo* ovarian cancer models and the underlying mechanisms of action remain to be elucidated.

The present study was undertaken to determine the molecular mechanisms of silibinin in human ovarian cancer cells *in vitro* and to examine *in vivo* efficacy of silibinin in a subcutaneous ovarian cancer animal model. Our data demonstrated that silibinin induces human ovarian cancer cell death via a reactive oxygen species (ROS)-associated downregulation of extracellular signal-regulated kinase (ERK) and Akt *in vitro* and causes dramatic regression of tumor growth *in vivo*.

Received: January 18, 2013

Revised: April 9, 2013

Accepted: April 9, 2013

Published: April 9, 2013

MATERIALS AND METHODS

Reagents. Silibinin, *N*-acetylcysteine (NAC), 3-[4,5-dimethylthiazol-2-yl]-2,5-diphenyltetrazolium bromide (MTT), Hoechst 33258, and propidium iodide were purchased from Sigma-Aldrich Chemical (St. Louis, MO). Tween 20 was purchased from Calbiochem (San Diego, CA). 2',7'-Dichlorofluorescein diacetate (DCFH-DA) was obtained from Molecular Probes (Eugene, OR). Antibodies were obtained from Cell Signaling Technology, Inc. (Beverly, MA). All other chemicals were of the highest commercial grade available.

Cell Culture. A2780 and SKOV3 cells were obtained from the American Type Culture Collection (Rockville, MD) and maintained by serial passages in 75 cm² culture flasks (Costar, Cambridge, MA). The cells were grown in Dulbecco's modified Eagle's medium (DMEM, Gibco BRL, Invitrogen, Carlsbad, CA) containing 10% heat-inactivated fetal bovine serum (HyClone, Logan, UT) at 37 °C in a humidified 95% air/5% CO₂ incubator.

Normal ovarian surface epithelial (OSE) cells were provided by Dr. Gil Mor (Yale University, New Haven, CT) and cultured in a 1:1 mixture of Medium 199 (WelGENE, Inc.) and MCDB 105 medium (WelGENE, Inc.), supplemented with 15% fetal bovine serum, penicillin/streptomycin (100 and 100 µg/mL), and L-glutamine (1 mM final concentration) at 37 °C in a 95% air and 5% CO₂ incubator.

When the cultures reached confluence, a subculture was prepared using a 0.02% ethylenediaminetetraacetic acid dipotassium salt dehydrate (EDTA)–0.05% trypsin solution. The cells were grown on 96-well tissue culture plates and used 1–2 days after plating when a 70–80% confluent monolayer culture was achieved. Cells were treated with silibinin in serum-free medium for 24 and 48 h. NAC was added to the medium 30 min before silibinin exposure.

Measurement of Cell Viability. Cell viability was evaluated using a MTT assay.¹⁴ Culture medium containing 0.5 mg/mL MTT was added to each well. The cells were incubated for 2 h at 37 °C. The supernatant was removed, and the formed formazan crystals in viable cells were solubilized with 0.1 mL of dimethyl sulfoxide. A 0.1 mL aliquot of each sample was then transferred to 96-well plates, and the absorbance of each well was measured at 550 nm with a ELISA Reader (FLUOstar OPTIMA, BMG LABTECH, Offenburg, Germany). Data were expressed as a percentage of the control measured in the absence of silibinin.

Annexin V Staining Assay. Phosphatidylserine exposure on the outer layer of the cell membrane was measured using the binding of annexin V–fluorescein isothiocyanate (FITC). Cells were harvested and washed with cold phosphate-buffered saline (PBS). The cells were incubated for 15 min with annexin V–FITC and propidium iodide and were analyzed by flow cytometry (Becton Dickinson, Franklin Lakes, NJ).

Measurement of Reactive Oxygen Species (ROS). The intracellular generation of ROS was measured using DCFH-DA. The non-fluorescent ester penetrates into the cells and is hydrolyzed to 2',7'-dichlorofluorescein (DCFH) by the cellular esterases. The probe (DCFH) is rapidly oxidized to the highly fluorescent compound 2',7'-dichlorofluorescein (DCF) in the presence of cellular peroxidase and ROS, such as hydrogen peroxide or fatty acid peroxides; thus, the fluorescence intensity is proportional to the amount of ROS produced by the cells. Cells cultured in 24-well plates were preincubated in the culture medium with 30 µM DCFH-DA for 1 h at 37 °C. After preincubation, the cells were exposed to 50 µM silibinin for indicated times. Changes in DCF fluorescence were assayed using a FACSort Becton Dickinson flow cytometer (Becton-Dickinson Bioscience, San Jose, CA), and data were analyzed with CELLQuest Software. Each measurement of ROS was performed 3 times in duplicate for calculation of the mean fluorescent intensity, which represents the amount of ROS generation. The mean fluorescent intensity was plotted along the y axis in panels A and B of Figure 2.

Western Blot Analysis. Cells were harvested after silibinin treatment and disrupted in lysis buffer [1% Triton X-100, 1 mM ethylene glycol-bis(β-aminoethyleter)-*N,N,N',N'*-tetraacetic acid (EGTA), 1 mM EDTA, 10 mM Tris-HCl at pH 7.4]. Cell debris was removed by centrifugation at 10000g for 10 min at 4 °C. The

resulting supernatants were resolved on a 10% sodium dodecyl sulfate–polyacrylamide gel electrophoresis (SDS–PAGE) under denatured reducing conditions and transferred to nitrocellulose membranes. The membranes were blocked with 5% nonfat dried milk at room temperature for 30 min and incubated with primary antibodies. The membranes were washed and incubated with horseradish peroxidase-conjugated secondary antibodies. The signal was visualized using enhanced chemiluminescence (Amersham, Buckinghamshire, U.K.).

Transfection of Constitutively Active Form of MEK (caMEK) and Akt (caAkt). Constitutively active forms of MEK and Akt were kindly provided by Dr. P. G. Suh (POSTECH, Pohang, Korea). A 2 µg cDNA sample was transiently transfected using Lipofectamine (Invitrogen) according to the guidelines of the manufacturer. After 4 h of incubation at 37 °C, cells were maintained in normal culture media for 24 h. In these experiments, cells transfected with an empty vector were employed as a control.

In Vivo Tumor Growth Assay. A2780 cells (3 × 10⁶) were injected subcutaneously into the right hind leg of 4-week-old female Balb/c nude mice. After injection, animals were fed with 50 and 100 mg/kg doses of silibinin (*n* = 5) in 50 µL of saline or with 50 µL of saline (vehicle; *n* = 5) by oral gavage daily. After 8 weeks, tumors were excised and tumor volume was calculated using the following equation: tumor volume (mm³) = (length × width²) × π/6.¹⁵ Tumors were fixed in formalin, embedded in paraffin, and sectioned by standard methods for immunohistochemical analyses.

Immunohistochemistry. Excised tumors were fixed in 4% (v/v) paraformaldehyde in PBS and embedded in paraffin. The tumor samples were subjected to antigen retrieval with 10 mM sodium citrate buffer (pH 6.0) for 10 min and blocked with 8% bovine serum albumin (BSA; Sigma) for 1 h. For immunostaining, sections were incubated overnight at 4 °C with rabbit polyclonal anti-Ki-67 (1:1000 dilution), anti-p-ERK (1:500 dilution), anti-p-Akt (1:500 dilution), and anti-caspase-3 (1:500 dilution) antibodies. The anti-Ki-67 sections were then incubated with appropriate fluorescein (FITC) secondary antibody for 1 h. Sections were stained with Hoechst 33258 for 15 min. For Ki-67 expression, a minimum of 400 cells were counted on one section per mouse and expressed as the number of positive cells at a magnification of 400X. Other sections were followed by biotinylated anti-rat IgG (Vector Laboratories, Burlingame, CA), and staining was visualized using biotin–avidin–peroxidase complexes (Vector Laboratories) and diaminobenzidine (Vector Laboratories). Slides were counter-stained with hematoxylin to allow for visualization of nuclei. The diaminobenzidine (DAB)-positive cells were measured by the color deconvolution plugin for ImageJ (NIH Image) and evaluated as the percentage of area.

Terminal Deoxynucleotidyl Transferase-Mediated dUTP Nick End Labeling (TUNEL) Assay. The TUNEL assay was performed using an In Situ Cell Death Detection Kit (Roche, IN) according to the instructions of the manufacturer, and pictures were taken on an inverted fluorescence microscope. Briefly, slides were deparaffinized and treated with permeabilization solution (0.1% Triton X-100 + 0.1% sodium citrate) at 4 °C for 2 min to enhance the staining. For detection of single- and double-stranded DNA breaks, slides were incubated for 1 h at 37 °C with a TUNEL reaction mixture (enzyme solution + labeling solution). Sections were stained with Hoechst 33258 for 15 min. The TUNEL-positive cells were counted and expressed as the percentage of total cells.

Statistical Analysis. The data were expressed as the mean ± standard error of the mean (SEM), and the difference between two groups was evaluated using the unpaired *t* test. Multiple group comparison was performed using one-way analysis of variance followed by Tukey's post-hoc test. A probability level of 0.05 was used to establish significance.

RESULTS

Antiproliferative Effect of Silibinin on Ovarian Cancer Cells. To determine the effect of silibinin on human ovarian cancer cells, A2780 and SKOV3 cells were exposed to various

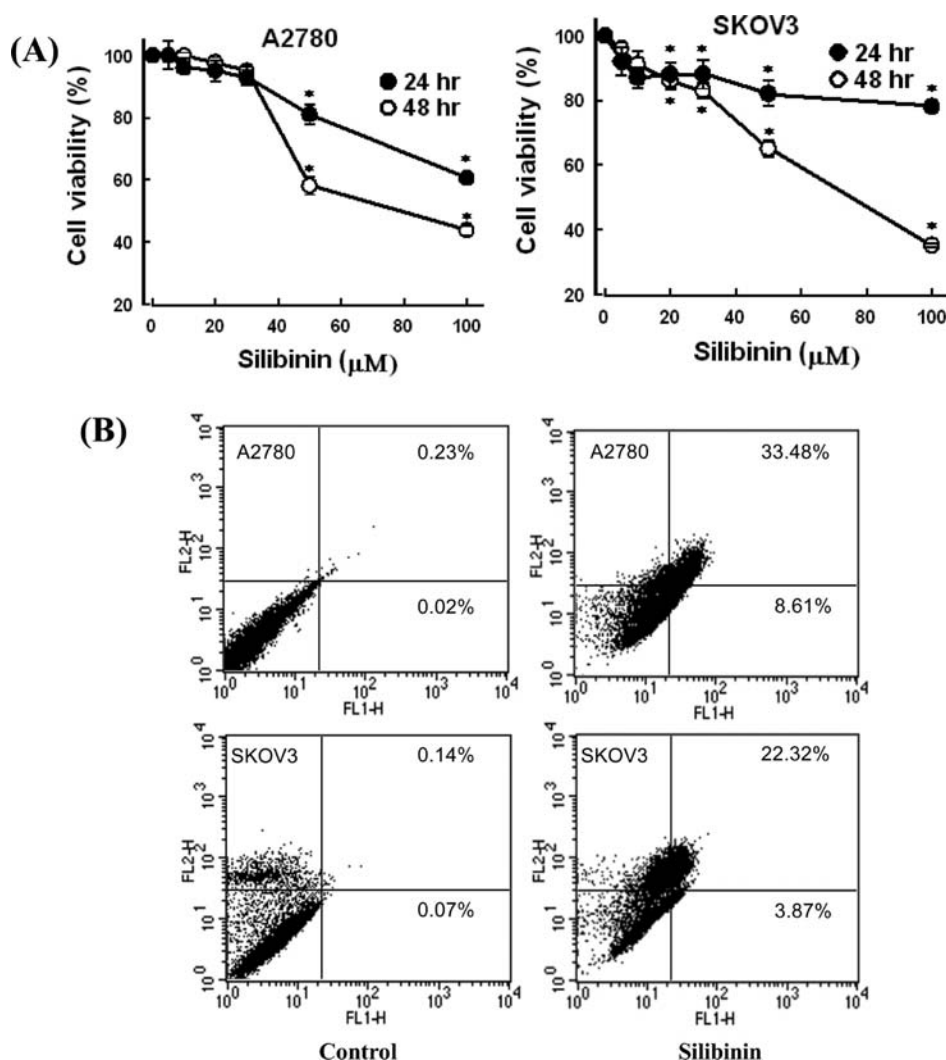


Figure 1. Effect of silibinin on cell viability and apoptosis. (A) A2780 and SKOV3 cells were exposed to 50 μM silibinin for 24 and 48 h. Cell viability was estimated by the MTT assay. Data are the mean \pm SEM of four independent experiments performed in duplicate. (*) $p < 0.05$ compared to the control without silibinin. (B) Cells were exposed to 50 μM silibinin for 48 h, stained with FITC-conjugated annexin V, and quantified by flow cytometric analysis. Numbers indicate the percentage of cells in each quadrant. Early apoptotic and late apoptotic cells were shown in the right lower and right upper quadrants, respectively.

concentrations of silibinin for 24 and 48 h. As shown in Figure 1, silibinin decreased cell viability in a time- and dose-dependent manner, with similar patterns in both cell types. Silibinin induced approximately 58–65% of cell viability at 50 μM after 48 h of exposure. In subsequent experiments, therefore, we exposed cells to 50 μM silibinin for 48 h.

To determine whether the reduction in cell viability was due to apoptosis, an annexin V binding assay was performed. Silibinin treatment increased apoptosis from 0.25% in the control to 42.09% and from 0.21 to 26.19% in A2780 and SKOV3 cells, respectively (Figure 1B). These results indicate that silibinin-induced reduction in cell viability is largely due to apoptosis.

We next examined the effect of silibinin on cell viability in the normal ovarian epithelial cells (OSE). Silibinin did not induce significant changes in cell viability even after exposure of 50 μM for 48 h (MTT assay: $98.80 \pm 3.37\%$ of the control; $n = 4$).

Role of ROS Generation in Silibinin-Induced Cell Death. To determine whether silibinin induces ROS generation in human ovarian cancer cells, A2780 and SKOV3

cells were exposed to silibinin for 24 and 48 h and changes in DCF fluorescence were measured. Silibinin caused a significant increase in ROS generation after silibinin treatment in both cell types (panels A and B of Figure 2).

To ascertain whether ROS generation is involved in the silibinin-induced cell death, the cell viability after the addition of antioxidant NAC was measured. The silibinin-induced cell death was prevented by the addition of NAC (Figure 2C), suggesting that the silibinin-induced cell death is associated with ROS generation in human ovarian cancer cells.

Role of ERK and Akt in Silibinin-Induced Cell Death. ERK and Akt play a pivotal role in cell proliferation, differentiation, and survival.^{16–18} If these kinases are down-regulated by silibinin, cell death could be induced. To assess this possibility, activities of these kinases were evaluated by detecting their phosphorylation forms. Cells were exposed to silibinin for indicated times, and changes in the phosphorylation of ERK and Akt were estimated by western blot analysis using antibodies specific to the respective phosphorylated form. Silibinin treatment caused a decrease in phosphorylation of these kinases (panels A and B of Figure 3).

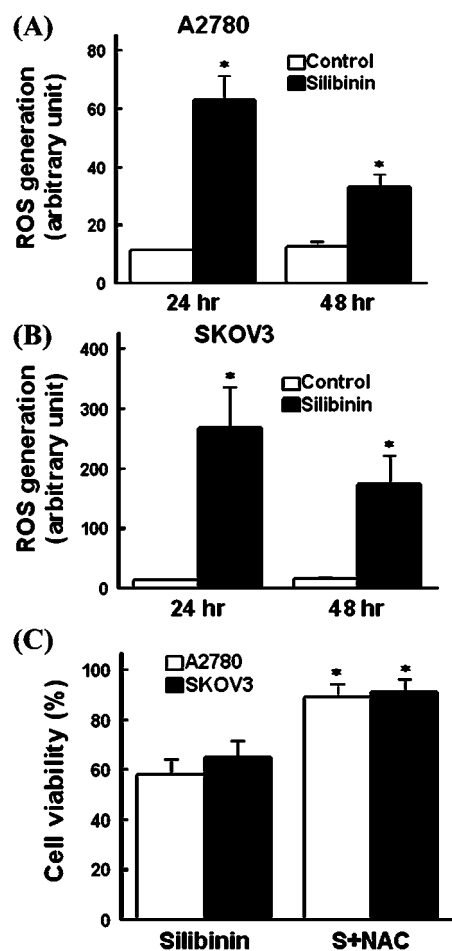


Figure 2. Role of ROS generation in silibinin-induced cell death. (A) A2780 and (B) SKOV3 cells were loaded with DCFH-DA for 1 h and treated with 50 μM silibinin for 24 and 48 h. DCF fluorescence intensity was measured by flow cytometry. Data are the mean \pm SEM of three experiments performed in duplicate. (*) $p < 0.05$ compared to the control. (C) Cells were treated with 50 μM silibinin in the presence or absence of 2 mM NAC for 48 h. Cell viability was determined by the MTT assay. Data are the mean \pm SEM of four independent experiments performed in duplicate. (*) $p < 0.05$ compared to silibinin alone.

To evaluate whether downregulation of ERK and Akt is responsible for the silibinin-induced cell death, the effect of silibinin on cell viability was examined in cells transfected with constitutively active forms of MEK (caMEK), the upstream kinase of ERK, and Akt (caAkt). Transfection of caMEK and caAkt prevented effectively the silibinin-induced cell death (Figure 3C), suggesting that downregulation of ERK and Akt plays a critical role in the silibinin-induced cell death.

To ascertain whether the downregulation of ERK and Akt by silibinin is associated with ROS generation, the effect of antioxidant NAC on the downregulation of these kinases was examined. The silibinin-induced inhibition of ERK and Akt phosphorylation was blocked by NAC (Figure 3D). These results indicate that ROS generation may act upstream for the downregulation of ERK and Akt in ovarian cancer cells exposed to silibinin.

Effect of Silibinin on Ovarian Tumor Growth *in Vivo*.

To determine the antineoplastic effect of silibinin *in vivo*, A2780 cells were injected subcutaneously into Balb/c nude mice. After injection, silibinin or vehicle (saline) was given by oral gavage

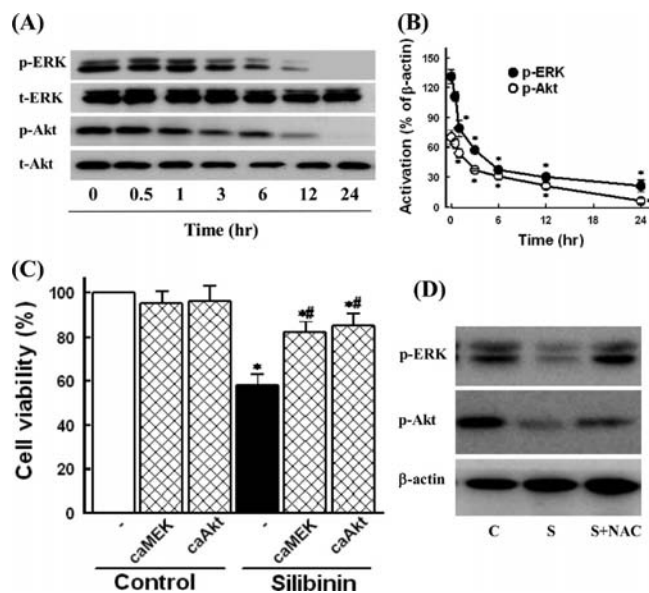


Figure 3. Role of ERK and Akt in silibinin-induced cell death. (A) A2780 cells were exposed to 50 μM silibinin for various times. Expression of phospho-ERK (p-ERK) and phospho-Akt (p-Akt) was evaluated using the specific antibodies. (B) Quantitative data of densitometric analysis. Data are the mean \pm SEM of three independent experiments. (*) $p < 0.05$ compared to the control. (C) A2780 cells were transfected with constitutively active forms of MEK (caMEK) and Akt (caAkt) and exposed to 50 μM silibinin for 48 h. Cell viability was estimated by the MTT assay. Data are the mean \pm SEM of four independent experiments performed in duplicate. (*) $p < 0.05$ compared to the control. (#) $p < 0.05$ compared to the empty vector. (D) A2780 cells were exposed to 50 μM silibinin in the presence or absence of 2 mM NAC for 24 h. Expression of p-ERK and p-Akt was evaluated by western blot analysis. C, control; S, silibinin; and NAC, *N*-acetylcysteine.

daily. Because previous studies have shown that doses of 100–200 mg/kg of silibinin exert antitumor effects in the animal model of colorectal cancer and human bladder cancer^{8,19} and glioblastoma,²⁰ animals were gavaged orally with 50 and 100 mg/kg doses of silibinin. All vehicle mice developed subcutaneous tumors with a volume of approximately 1166 mm³ after 8 weeks. In each case, the tumor volume in the silibinin-treated mice was significantly smaller than that of vehicle mice (panels A and B of Figure 4).

Effect of Silibinin on the Proliferation and Apoptosis *in Vivo*.

To assess whether silibinin inhibits tumor proliferation *in vivo*, Ki-67 expression was evaluated. Silibinin treatment decreased the proliferative rate of tumor cells (Figure 5). While A2780 cells from the vehicle mice showed almost no TUNEL-positive cells, tumor cells from mice treated with silibinin showed a marked increase in TUNEL-positive cells (Figure 6) and activation of caspase-3 (Figure 7), which indicated that silibinin induced apoptosis *in vivo*.

Effect of Silibinin on the Activation of ERK and Akt *in Vivo*.

To assess whether silibinin affects activation of ERK and Akt *in vivo*, phosphorylation of ERK and Akt was evaluated. Tumor tissues of animals treated with 50 mg/kg of silibinin alone were chosen for these studies, because tumor volume was too small in animals treated with 100 mg/kg of silibinin. Activation of ERK and Akt was apparent in tumor tissues of vehicle mice, which was significantly inhibited by silibinin treatment (Figure 7).

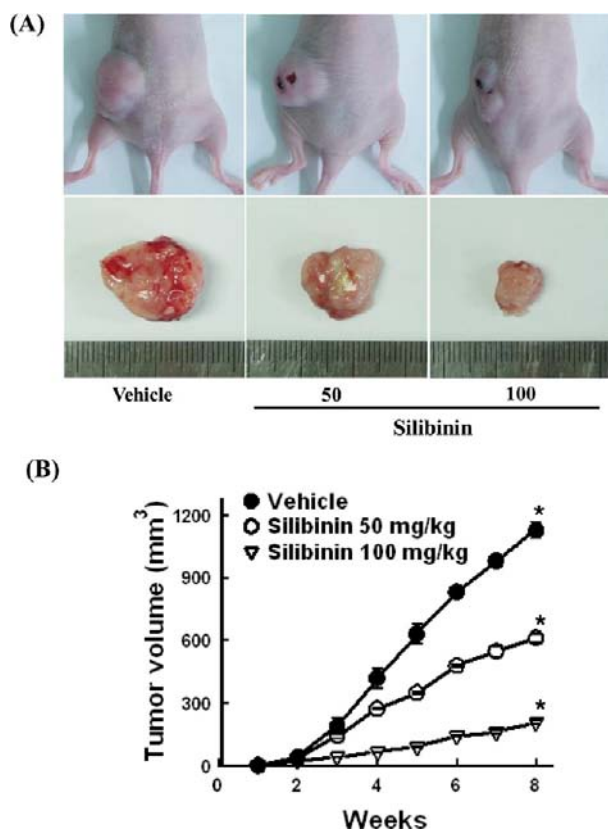


Figure 4. Effect of silibinin on ovarian tumor growth in Balb/c nude mice. A2780 cells (2×10^6) were injected subcutaneously into the right hind leg of 4-week-old female nude mice. After injection, silibinin (50 and 100 mg/kg) in 50 μ L of saline or with 50 μ L of saline (vehicle) was administered by oral gavage daily. The tumor volume was recorded weekly throughout experiments. After 8 weeks, the tumors were excised and tumor volume was calculated using the following equation: tumor volume (mm^3) = (length \times width²) \times $\pi/6$. Data in panel B are the mean \pm SEM of five animals in each group. (*) $p < 0.05$ compared to the vehicle group.

DISCUSSION

Although the antioxidant effect of flavonoids has been well-known,⁶ they may also behave as a pro-oxidant, generating ROS, which is responsible for cell death in some cancer cells.^{21–24} However, the role of ROS in the silibinin-induced cell death is not clear in human ovarian cancer cells. In the present study, silibinin increased ROS generation and the antioxidant NAC prevented the silibinin-induced cell death (Figure 2). These results indicate that the silibinin-induced cell death is possibly linked with ROS generation and are consistent with those reported in human glioma cells.²⁰ In our previous study,²⁰ we observed that silibinin induced cell death via a Ca^{2+} /ROS/MAPK-dependent mechanism in glioma cells. Silibinin caused an intracellular Ca^{2+} increase and ROS production. The silibinin-induced ROS generation was blocked by the addition of Ca^{2+} chelator EGTA, implying that silibinin causes ROS generation through a Ca^{2+} -dependent mechanism. Although we did not assess the role of Ca^{2+} in silibinin-induced ROS generation in the present study, one possible mechanism of ROS production by silibinin is through a Ca^{2+} -dependent mechanism in ovarian cancer cells. The detailed mechanism of silibinin-induced ROS generation is still not clear. p53 was found to be related to silibinin-induced ROS generation in fibrosarcoma HT1080 cells, melanoma A375-S2 cells, and

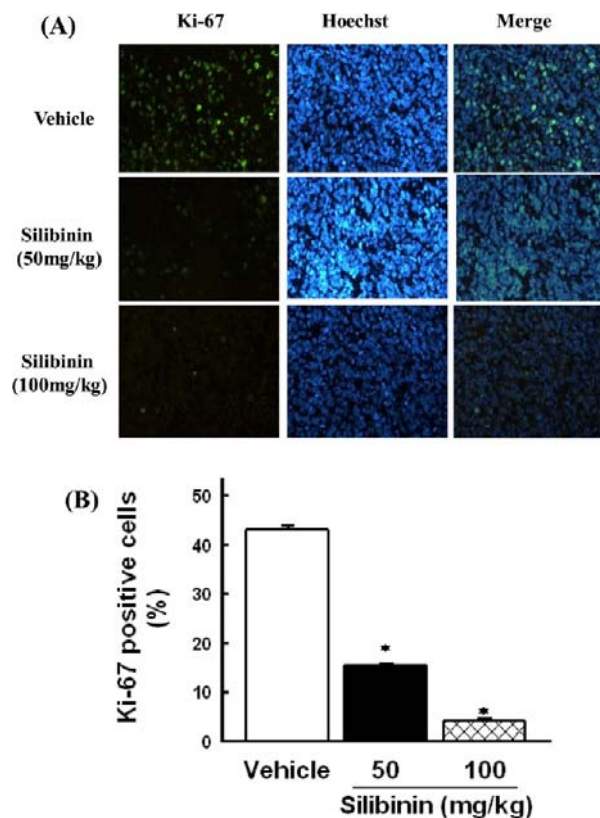


Figure 5. Effect of silibinin on cell proliferation in tumor tissues. Animals were sacrificed at 8 weeks after subcutaneous injection of A2780 cells. Tumor tissues were incubated with rabbit anti-Ki-67 at 4 $^{\circ}$ C overnight. Counterstaining was carried out with Hoechst 33258. The green color shows Ki-67-positive cells. (A) Representative and (B) quantitative results of five animals are shown. Data are the mean \pm SEM of five animals in each group. (*) $p < 0.05$ compared to the vehicle group.

breast cancer MCF-7 cells.^{25–27} Fan et al. suggested the JNK–p53–ROS pathway in silibinin-induced ROS generation in HeLa cells.²⁸

ERK is activated by a variety of extracellular signals, including mitogens, contributes to the proliferative responses in cells, and is considered to be an essential common element of mitogenic signaling.^{16,29} Its constitutive expression causes cell transformation and plays a putative role in carcinogenesis and drug resistance.³⁰ However, the effect of flavonoids on ERK activation is controversial. Activation of ERK is inhibited by flavonoids in vascular smooth muscle cells,³¹ human epidermal carcinoma cells,³² and neuronal cells,³³ whereas its activity is increased following flavonoid treatment in lung cancer cells.³⁴ Previously, we observed that ERK is activated by silibinin²⁰ and inhibited by kaempferol²⁴ in human glioma cells. These studies suggest that the effect of flavonoids on ERK activation may be dependent upon cell types and flavonoid structures. In the present study, silibinin caused an inhibition of ERK phosphorylation (panels A and B of Figure 3) and the silibinin-induced cell death was prevented by overexpression of ERK (Figure 3C). These data imply that downregulation of ERK signaling pathway plays an important role in the silibinin-induced cell death in ovarian cancer cells.

The Akt signaling pathway plays a critical role in the transmission of signals from growth factor receptors to regulate gene expression and prevent apoptosis. The relationship

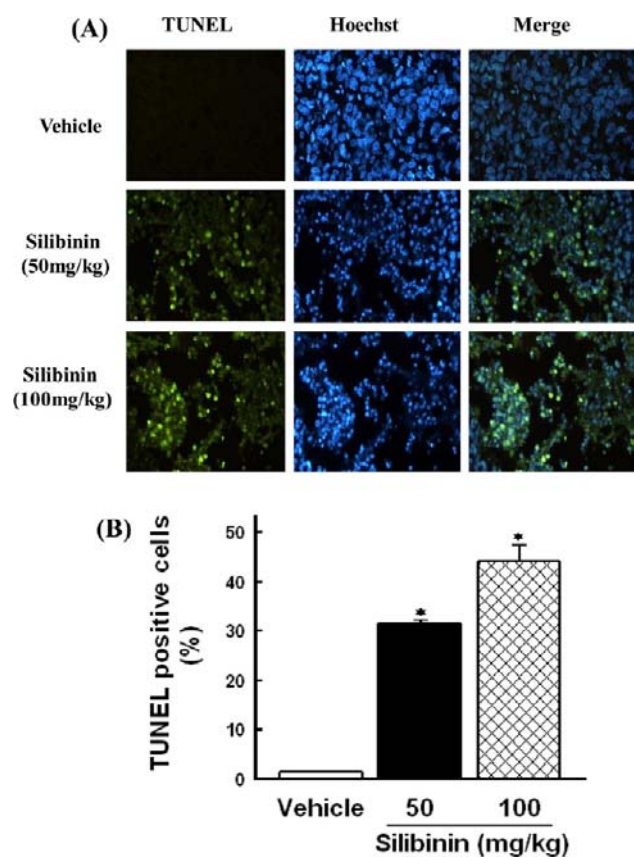


Figure 6. Effect of silibinin on apoptosis in tumor tissues. Animals were sacrificed at 8 weeks after subcutaneous injection of A2780 cells, and tumor tissues were sectioned. Apoptosis (green) was estimated with the TUNEL assay using an In Situ Cell Death Detection Kit. (A) Representative and (B) quantitative results of five animals are shown. Data are the mean \pm SEM of five animals in each group. (*) $p < 0.05$ compared to the vehicle group.

between dysregulated Akt activity and the initiation of cancer is well-documented.³⁵ It has been reported that the aberrant activation of Akt signaling in ovarian cancer may be used as a predictive marker of patient outcomes.³⁶ Therefore, regulation of the Akt signaling pathway may be a promising target for the clinical management of ovarian cancers. In the present study, Akt was highly activated in A2780 cells, and the Akt activation was inhibited by silibinin (panels A and B of Figure 3). The silibinin-induced cell death was also prevented by transfection of caAkt (Figure 3C). These data imply that silibinin induces ovarian cancer cell death through inhibition of the Akt pathway.

ROS induces the activation of multiple signaling pathways, including Akt and ERK, leading to cell survival or cell death.³⁷ On the other hand, the ability of ROS to trigger downregulation of the ERK and Akt pathway has also been reported.^{38,39} In the present study, inhibition of Akt and ERK by silibinin was blocked by the antioxidant NAC (Figure 3D), suggesting that ROS generation may act upstream of the downregulation of ERK and Akt.

To evaluate the antineoplastic effect of silibinin *in vivo*, tumor growth after subcutaneous implantation of A2780 cells was examined in nude mice. Oral silibinin administration markedly reduced tumor volume (Figure 4). Silibinin treatment also caused inhibition of cell proliferation and induction of apoptosis, as evidenced by a decrease in Ki-67-positive cells (Figure 5), an increase in TUNEL-positive cells (Figure 6), and

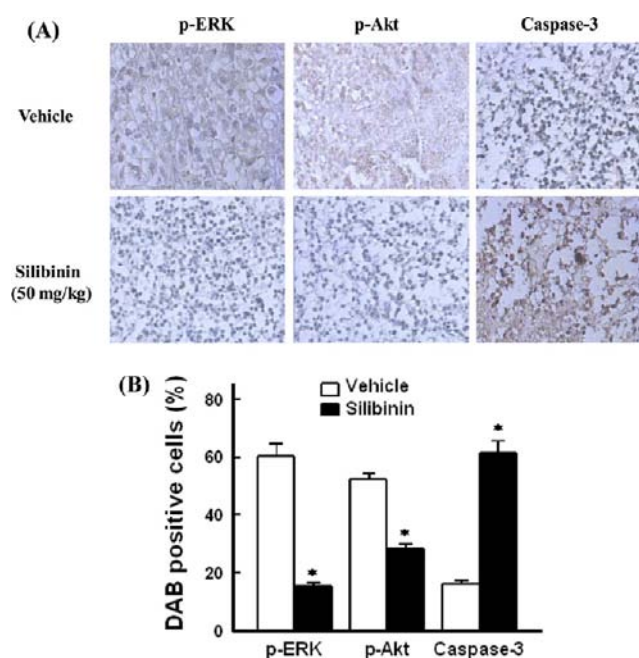


Figure 7. Effect of silibinin on activation of phospho-ERK (p-ERK), phospho-Akt (p-Akt), and caspase-3 in tumor tissues. Animals were sacrificed at 8 weeks after subcutaneous injection of A2780 cells. Tumor tissues of animals treated with 50 mg/kg of silibinin were incubated with anti-p-ERK, anti-p-Akt, and anti-caspase-3 antibody, followed by biotinylated anti-rat IgG, and staining was visualized using biotin-avidin-peroxidase complexes and diaminobenzidine. Slides were counter-stained with hematoxylin to allow for visualization of nuclei. DAB-positive cells were measured by the color deconvolution plugin for ImageJ. Data are the mean \pm SEM of five animals in each group. (*) $p < 0.05$ compared to the vehicle group.

caspase-3 activation (Figure 7). Silibinin treatment caused the downregulation of ERK and Akt phosphorylation *in vivo* (Figure 7).

The concentration of silibinin in the blood after oral gavage was not provided in this study. An assay that can accurately quantify the concentration of silibinin in the blood is necessary for proper pharmacokinetic analysis. Wu et al.⁴⁰ reported that the absolute oral bioavailability of silibinin in rats was calculated to be about 0.95%. After silibinin administration in rats, the disposition of silibinin in the plasma and bile fluid was due to rapid distribution and equilibration between the blood and hepatobiliary system, and the bile levels of unconjugated silibinin and total silibinin were greater than those in the plasma.

Taken together, the results of the present study demonstrated that silibinin inhibits ovarian tumor growth through inhibition of proliferation and induction of apoptosis. ERK and Akt signaling pathways play a critical role in the antineoplastic action of silibinin. A further study to understand better the cytotoxicity of silibinin is required in ovarian tumor xenograft through the blood biomarker assay. The data that we present herein suggest that silibinin may be considered a potential candidate in the treatment of human ovarian cancers.

■ AUTHOR INFORMATION

Corresponding Author

*Telephone: 82-51-510-8070. Fax: 82-51-510-8076. E-mail: ghkim@pusan.ac.kr.

Author Contributions

†These authors contributed equally to this work.

Funding

This study was supported by a grant from the National R&D Program for Cancer Control, Ministry for Health, Welfare and Family Affairs, Republic of Korea (0920050).

Notes

The authors declare no competing financial interest.

REFERENCES

- (1) Schwartz, P. E. Current diagnosis and treatment modalities for ovarian cancer. *Cancer Treat. Res.* **2002**, *107*, 99–118.
- (2) Heintz, A. P.; Odicino, F.; Maisonneuve, P.; Quinn, M. A.; Benedet, J. L.; et al. Carcinoma of the ovary. FIGO 26th Annual Report on the Results of Treatment in Gynecological Cancer. *Int. J. Gynaecol. Obstet.* **2006**, *95*, S161–192.
- (3) Pignata, S.; Cannella, L.; Leopardo, D.; Pisano, C.; Bruni, G. S.; et al. Chemotherapy in epithelial ovarian cancer. *Cancer Lett.* **2011**, *303* (2), 73–83.
- (4) Ramos, S. Effects of dietary flavonoids on apoptotic pathways related to cancer chemoprevention. *J. Nutr. Biochem.* **2007**, *18* (7), 427–442.
- (5) Kanadaswami, C.; Lee, L. T.; Lee, P. P.; Hwang, J. J.; Ke, F. C.; et al. The antitumor activities of flavonoids. *In Vivo* **2005**, *19* (5), 895–909.
- (6) Ren, W.; Qiao, Z.; Wang, H.; Zhu, L.; Zhang, L. Flavonoids: Promising anticancer agents. *Med. Res. Rev.* **2003**, *23* (4), S19–S34.
- (7) Fresco, P.; Borges, F.; Diniz, C.; Marques, M. P. New insights on the anticancer properties of dietary polyphenols. *Med. Res. Rev.* **2006**, *26* (6), 747–766.
- (8) Singh, R. P.; Gu, M.; Agarwal, R. Silibinin inhibits colorectal cancer growth by inhibiting tumor cell proliferation and angiogenesis. *Cancer Res.* **2008**, *68* (6), 2043–2050.
- (9) Singh, R. P.; Mallikarjuna, G. U.; Sharma, G.; Dhanalakshmi, S.; Tyagi, A. K.; et al. Oral silibinin inhibits lung tumor growth in athymic nude mice and forms a novel chemocombination with doxorubicin targeting nuclear factor κ B-mediated inducible chemoresistance. *Clin. Cancer Res.* **2004**, *10* (24), 8641–8647.
- (10) Ramasamy, K.; Agarwal, R. Multitargeted therapy of cancer by silymarin. *Cancer Lett.* **2008**, *269*, 352–362.
- (11) Kaur, M.; Agarwal, R. Silymarin and epithelial cancer chemoprevention: How close we are to bedside? *Toxicol. Appl. Pharmacol.* **2007**, *224* (3), 350–359.
- (12) Zhou, L.; Liu, P.; Chen, B.; Wang, Y.; Wang, X.; et al. Silibinin restores paclitaxel sensitivity to paclitaxel-resistant human ovarian carcinoma cells. *Anticancer Res.* **2008**, *28* (2A), 1119–1127.
- (13) Giacomelli, S.; Gallo, D.; Apollonio, P.; Ferlini, C.; Distefano, M.; et al. Silybin and its bioavailable phospholipid complex (IdB 1016) potentiate in vitro and in vivo the activity of cisplatin. *Life Sci.* **2002**, *70* (12), 1447–1459.
- (14) Denizot, F.; Lang, R. Rapid colorimetric assay for cell growth and survival. Modifications to the tetrazolium dye procedure giving improved sensitivity and reliability. *J. Immunol. Methods* **1986**, *89* (2), 271–277.
- (15) Suzuki, E.; Kim, S.; Cheung, H. K.; Corbley, M. J.; Zhang, X.; Sun, L.; et al. A novel small-molecule inhibitor of transforming growth factor β type I receptor kinase (SM16) inhibits murine mesothelioma tumor growth in vivo and prevents tumor recurrence after surgical resection. *Cancer Res.* **2007**, *67* (5), 2351–2359.
- (16) Xia, Z.; Dickens, M.; Raingeaud, J.; Davis, R. J.; Greenberg, M. E. Opposing effects of ERK and JNK-p38 MAP kinases on apoptosis. *Science* **1995**, *270* (5240), 1326–1331.
- (17) Cobb, M. H. MAP kinase pathways. *Prog. Biophys. Mol. Biol.* **1999**, *71* (3–4), 479–500.
- (18) Coffey, P. J.; Jin, J.; Woodgett, J. R. Protein kinase B (c-Akt): A multifunctional mediator of phosphatidylinositol 3-kinase activation. *Biochem. J.* **1998**, *335*, 1–13.
- (19) Singh, R. P.; Tyagi, A.; Sharma, G.; Mohan, S.; Agarwal, R. Oral silibinin inhibits in vivo human bladder tumor xenograft growth involving down-regulation of survivin. *Clin. Cancer Res.* **2008**, *14* (1), 300–308.
- (20) Kim, K. W.; Choi, C. H.; Kim, T. H.; Kwon, C. H.; Woo, J. S.; et al. Silibinin inhibits glioma cell proliferation via Ca^{2+} /ROS/MAPK-dependent mechanism in vitro and glioma tumor growth in vivo. *Neurochem. Res.* **2009**, *34* (8), 1479–1490.
- (21) Chen, Y. C.; Shen, S. C.; Chow, J. M.; Ko, C. H.; Tseng, S. W. Flavone inhibition of tumor growth via apoptosis in vitro and in vivo. *Int. J. Oncol.* **2004**, *25* (3), 661–670.
- (22) Wang, I. K.; Lin-Shiau, S. Y.; Lin, J. K. Induction of apoptosis by apigenin and related flavonoids through cytochrome *c* release and activation of caspase-9 and caspase-3 in leukaemia HL-60 cells. *Eur. J. Cancer* **1999**, *35* (10), 1517–1525.
- (23) Kim, E. J.; Choi, C. H.; Park, J. Y.; Kang, S. K.; Kim, Y. K. Underlying mechanism of quercetin-induced cell death in human glioma cells. *Neurochem. Res.* **2008**, *33* (6), 971–979.
- (24) Jeong, J. C.; Kim, M. S.; Kim, T. H.; Kim, Y. K. Kaempferol induces cell death through ERK and Akt-dependent down-regulation of XIAP and survivin in human glioma cells. *Neurochem. Res.* **2009**, *34* (5), 991–1001.
- (25) Duan, W.; Jin, X.; Li, Q.; Tashiro, S.; Onodera, S.; Ikejima, T. Silibinin induced autophagic and apoptotic cell death in HT1080 cells through a reactive oxygen species pathway. *J. Pharmacol. Sci.* **2011**, *113*, 48–56.
- (26) Jiang, Y. Y.; Yang, R.; Wang, H. J.; Huang, H.; Wu, D.; Tashiro, S. I.; et al. Mechanism of autophagy induction and role of autophagy in antagonizing mitomycin C-induced cell apoptosis in silibinin treated human melanoma A375-S2 cells. *Eur. J. Pharmacol.* **2011**, *668*, 78–87.
- (27) Noh, E. M.; Yi, M. S.; Youn, H. J.; Lee, B. K.; Lee, Y. R.; Han, J. H.; et al. Silibinin enhances ultraviolet B-induced apoptosis in mcf-7 human breast cancer cells. *Int. J. Breast Cancer* **2011**, *14*, 8–13.
- (28) Fan, S.; Qi, M.; Yu, Y.; Li, L.; Yao, G.; Tashiro, S.; et al. P53 activation plays a crucial role in silibinin induced ROS generation via PUMA and JNK. *Free Radical Res.* **2012**, *46* (3), 310–319.
- (29) Pearson, G.; Robinson, F.; Beers Gibson, T.; Xu, B. E.; Karandikar, M.; et al. Mitogen-activated protein (MAP) kinase pathways: Regulation and physiological functions. *Endocr. Rev.* **2001**, *22* (2), 153–183.
- (30) McCubrey, J. A.; Steelman, L. S.; Chappell, W. H.; Abrams, S. L.; Wong, E. W.; et al. Roles of the Raf/MEK/ERK pathway in cell growth, malignant transformation and drug resistance. *Biochim. Biophys. Acta* **2007**, *1773* (8), 1263–1284.
- (31) Moon, S. K.; Cho, G. O.; Jung, S. Y.; Gal, S. W.; Kwon, T. K.; et al. Quercetin exerts multiple inhibitory effects on vascular smooth muscle cells: Role of ERK1/2, cell-cycle regulation, and matrix metalloproteinase-9. *Biochem. Biophys. Res. Commun.* **2003**, *301* (4), 1069–1078.
- (32) Singh, R. P.; Tyagi, A. K.; Zhao, J.; Agarwal, R. Silymarin inhibits growth and causes regression of established skin tumors in SENCAR mice via modulation of mitogen-activated protein kinases and induction of apoptosis. *Carcinogenesis* **2002**, *23* (3), 499–510.
- (33) Spencer, J. P.; Rice-Evans, C.; Williams, R. J. Modulation of pro-survival Akt/protein kinase B and ERK1/2 signaling cascades by quercetin and its in vivo metabolites underlie their action on neuronal viability. *J. Biol. Chem.* **2003**, *278* (37), 34783–34793.
- (34) Nguyen, T. T.; Tran, E.; Nguyen, T. H.; Do, P. T.; Huynh, T. H.; et al. The role of activated MEK-ERK pathway in quercetin-induced growth inhibition and apoptosis in A549 lung cancer cells. *Carcinogenesis* **2004**, *25* (5), 647–659.
- (35) McCubrey, J. A.; Steelman, L. S.; Abrams, S. L.; Lee, J. T.; Chang, F.; et al. Roles of the RAF/MEK/ERK and PI3K/PTEN/AKT pathways in malignant transformation and drug resistance. *Adv. Enzyme Regul.* **2006**, *46*, 249–279.
- (36) Huang, J.; Zhang, L.; Greshock, J.; Colligon, T. A.; Wang, Y.; et al. Frequent genetic abnormalities of the PI3K/AKT pathway in primary ovarian cancer predict patient outcome. *Genes, Chromosomes Cancer* **2011**, *50* (8), 606–618.

(37) Martindale, J. L.; Holbrook, N. J. Cellular response to oxidative stress: Signaling for suicide and survival. *J. Cell Physiol.* **2002**, *192*, 1–15.

(38) Yang, H. Y.; Kim, J.; Chung, G. H.; Lee, J. C.; Jang, Y. S. Cross-linking of MHC class II molecules interferes with phorbol 12,13-dibutyrate-induced differentiation of resting B cells by inhibiting Rac-associated ROS-dependent ERK/p38 MAP kinase pathways leading to NF- κ B activation. *Mol. Immunol.* **2007**, *44* (7), 1577–1586.

(39) Su, Y. T.; Chang, H. L.; Shyue, S. K.; Hsu, S. L. Emodin induces apoptosis in human lung adenocarcinoma cells through a reactive oxygen species-dependent mitochondrial signaling pathway. *Biochem. Pharmacol.* **2005**, *70* (2), 229–241.

(40) Wu, J. W.; Lin, L. C.; Hung, S. C.; Chi, C. W.; Tsai, T. H. Analysis of silibinin in rat plasma and bile for hepatobiliary excretion and oral bioavailability application. *J. Pharm. Biomed. Anal.* **2007**, *45*, 635–641.